Exploring the Formation and Evolution of Planetary Systems
Proceedings IAU Symposium No. 299, 2013
M. Booth, B. C. Matthews & J. R. Graham, eds.

doi:10.1017/S1743921313008326

Orbital Motion and Multi-Wavelength Monitoring of LkCa15 b

Michael J. Ireland[1,2] **and Adam L. Kraus**[3,4]

[1]Australian Astronomical Observatory, PO Box 296, Epping NSW 1710, Australia
email: `mireland@aao.gov.au`

[2]Department of Physics & Astronomy, Macquarie University, NSW 2109 Australia

[3]Department of Astronomy, University of Texas at Austin,
2515 Speedway, Stop C1400 Austin, Texas 78712-1205, USA
email: `alk@astro.as.utexas.edu`

[4]Harvard-Smithsonian Center for Astrophysics, 60 Garden St, Cambridge, MA 02138, USA

Abstract. As part of a deep multi-year non-redundant aperture mask infrared imaging campaign observing transition disks, we present multi-epoch monitoring of the resolved emission seen within the disk gap of LkCa 15. Orbital motion of both the central source and extended lobes as presented in Kraus and Ireland (2012) is clearly detected at the level of ∼4 degrees/year (deprojected), in both K and L'-bands. Based on these data as well as single-epoch H and M bands epochs, we present two models for the central source - thermal emission as a planetary accretion signature and scattering. The thermal emission model is preferred.

Keywords. planets and satellites: formation, stars: individual: LkCa 15, instrumentation: high angular resolution, techniques: image processing

---

1. Introduction

Since the discovery of the first hot jupiter planet (Mayor and Queloz 1995) it has been clear that orbital evolution plays an important role in the configuration of mature planetary systems. Understanding planetary formation therefore requires not only a census of mature systems, but also direct detection of planets as they are forming. Luckily, the bulk of the gravitational potential energy of a forming giant planet is released early in its lifetime. This is especially true in the core-accretion model, where the release of energy in an accretion-shock can in principle radiate with a luminosity approaching $0.1\,L_\odot$ for $\sim 10^5$ years (Marley *et al.* 2007).

The greatest difficulty in directly detecting newly-formed exoplanets with current-generation telescopes is the relatively large distances to nearby star forming regions. In Taurus in the northern hemisphere or ρ Ophiucus in the southern hemisphere, a linear separation of 5 AU corresponds to only 0.035 arc sec, which is within the formal diffraction limit of the world's largest telescopes for all bandpasses longer than the H-band (1.55 μm).

Maximizing contrast at the diffraction-limit requires more than just an adaptive optics system. Fundamental noise sources such as photon-noise play only a small role in detecting faint companions. For example, a K = 20 object buried in the Airy ring of a K = 10 star, taken with a high-Strehl, 25% efficiency adaptive optics system on a 10m telescope would be detected with a photon-limited signal-to-noise of more than 5 in only 10 s. At this contrast level of 10^4, phase noise is the dominant error source – in particular, phase noise that manifests itself as quasi-static speckles. Techniques such as LOCI (Lafrenière *et al.* 2007), KL image projection (Soummer *et al.* 2012) and POISE (Ireland 2013) help to distinguish the signal of a companion from a phase-noise signal, but it

Table 1. Summary of LkCa 15 Observations with Keck.

Date	Filter	Observation Time	Detection?
2008 Dec	K'	0.5 hours	N
2009 Nov	L'	4 hours	Y
2010 Aug	L'	2 hours	Y
2010 Nov	K'	3.5 hours	Y
2010 Nov	L'	1.5 hours	Y
2012 Jan	H[1]	6 hours	N
2012 Jan	Ms	2 hours	Y
2012 Aug	L'	1.5 hours	N
2012 Dec	K'	3 hours	Y
2012 Dec	L'	1 hour	Y

Notes:
[1] Actually the CH4-short filter of NIRC2, comprising the short-wavelength half of the H-band.

also helps to define an observable that is least-affected by phase-noise. A coronagraph removes the diffracted electric field in the image-plane, making quasi-static speckles 2nd-order (rather than 1st-order) in pupil-plane phase errors. A technique even less sensitive to pupil-plane phase errors is *kernel-phase*, where detection thresholds are 3rd order in pupil-plane phase (Martinache 2012, Ireland 2012, Ireland 2013). In order for kernel-phase to be effective at moderate Strehl ratios, the pupil geometry also must be modified with an aperture-mask (Lloyd *et al.* 2006). It is the observable of kernel-phase, with or without an aperture-mask that we have used to maximise our sensitivity to exoplanets at the diffraction-limit of the world's largest telescopes (Keck and VLT).

2. Observations of Transition Disks

Detecting young exoplanets at solar-system scales requires not only the best technique but also a carefully constructed target list. We have been systematically targeting the so-called "transition" disks, which have a cleared inner-hole. For more massive disks where photo-evaporation can not yet play a significant role in disk shaping, the key clearing possible mechanisms are significant grain growth and dynamical interactions with forming protoplanets (Dodson-Robinson and Salyk 2011) or companions (Ireland and Kraus 2008). Significant grain growth is itself a signature that a disk is at a planet forming stage, so for disks that are not cleared by a stellar companion, a transition disk spectrum can be seen as a signpost for planetary formation.

We have carried out the deepest observations for transition disks with the L' filter at the Keck telescope, achieving typical contrast limits of 6 magnitudes. Our target list included UX Tau, GM Aur, LkCa 15, LkHa 330 and SR 21. Only one target showed an unambiguous sign of substructure within its disk gap, LkCa 15. This detection was published in Kraus and Ireland 2012.

3. New Observations of LkCa 15

The full set of Keck, NIRC2 observations of LkCa15 are given in Table 1. All 2012 observations are unpublished, with preliminary results first presented at this conference. The 2012 K-band epoch is shown in Figure 1, with a similar observing technique and image reconstruction technique to Kraus and Ireland (2012). The white circles in the image show the positions of the NE lobe, central source and SW lobe as presented in Kraus and Ireland (2012). The central source has approximately the same brightness between epochs, but the lobes are clearly brighter in 2012. L-band images (not shown) are consistent with similar levels of orbital motion and variability. When all data are taken

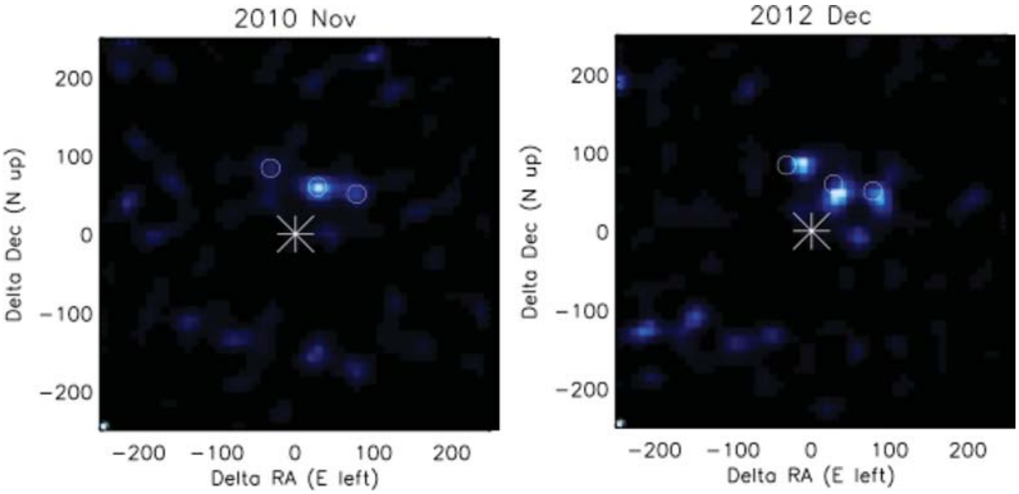

Figure 1. Image reconstructions from 2010 and 2012 data sets in K-band, showing clockwise orbital motion. Each image was reconstructed from closure-phase data only using the MACIM algorithm Ireland *et al.* 2006. Variability is also seen in the resolved structure to the NW of the central star (modelled as a point source).

together, we see orbital motion of 6.0 ± 1.5 degrees per year, which is approximately 4 degrees per year deprojected for a circular orbit once the system inclination of 49 degrees is taken into account. This is consistent with Keplerian rotation for at 20 AU orbit.

During 2012 Jan, we attempted to detect emission from LkCa 15b in H-band, using the 9-hole aperture mask of NIRC2 and the CH4-short filter. Including overheads and calibrations, 6 hours was spent on target, with no detections down to a contrast of 7 magnitudes. Figure 2 shows the reconstructed image from these observations: the noise peak in the NW corner would correspond to a companion with contrast of 7.2 magnitudes.

In the Ms filter, aperture-masking data has poor signal-to-noise because of both the light loss at the aperture-mask, and the sensitivity to thermal background due to the aperture-mask technique spreading information over a sky area ∼50 times larger than data with an unobstructed pupil. However, Strehl ratios are much higher in the Ms filter than K' and L', meaning that it is possible to use the Kernel-phase technique on data taken with an unobstructed pupil under most seeing conditions. The reconstructed image (Figure 2) has resolved structure at the same location as the K' and the L' filters, and a integrated contrast of 3.5 magnitudes.

4. Discussion

When taken together with the resolved velocity CO observations of Simon *et al.* (2000), the clockwise orbital motion means that the resolved emission is geometrically behind LkCa 15. In turn, this means that forward scattering can not be evoked as an emission mechanism to give an apparent albedo greater than unity. Given the L' contrast of the resolved structure of ∼4.5 magnitudes and the Ms contrast of the structure of 3.5 magnitudes, this in turn means that it is extremely difficult to explain the amount of emission from the resolved structure as scattering. The very red colors (K'-Ms color more than ∼1.5 magnitudes redder than the star) are also inconsistent with typical scattering processes, which typically have a blue or neutral colour.

This leaves thermal emission as the obvious explanation for the resolved structure. The K'-Ms color implies a temperature of 900K for small, optically-thin grains, or an even

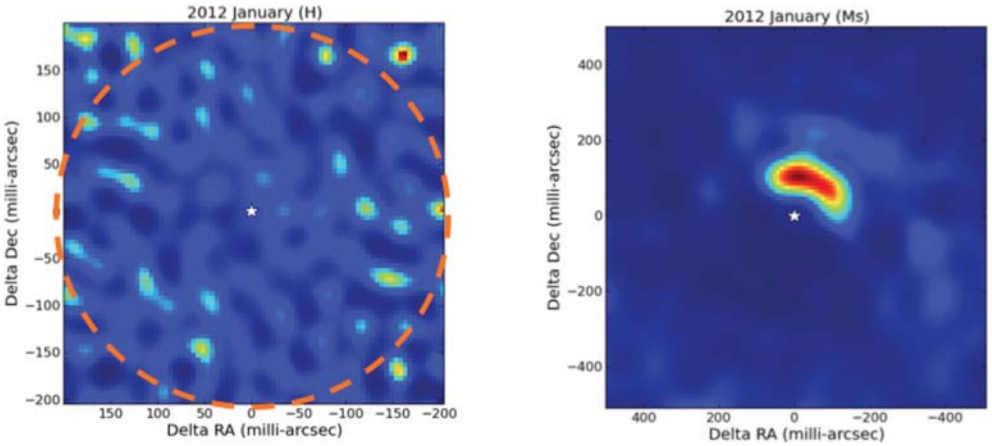

Figure 2. Image reconstructions from H-band (1.55 μm, left, no detection), and Ms-band (4.7 μm, right), with the star not shown (modelled as a central point source). The Maximum Entropy image reconstruction technique as described in Ireland(2013) was used, which images from both aperture-masking data (H-band) and kernel-phase data taken with an unobstructed telescope pupil (Ms filter). The dashed line shows the rough window size for the aperture-mask analysis in H-band. In M-band, the resolved structure has an integrated brightness approximately 3.5 magnitudes fainter than the central star.

higher temperature for optically-thick material. This is much higher than the $\sim$250 K maximum temperature for small grains at 20 AU separations in equilibrium with the stellar radiation field. The integrated luminosity of $3{\times}10^{-3}$ L$_\odot$ between 2 and 5 microns is also very high, and only consistent with the luminosity of the Marley *et al.* (2007) models for 1–3 M$_J$ masses for a period of $\sim 10^5$ years. This luminosity is therefore remains consistent with planetary formation, but the mechanism for producing the emission remains unknown.

References

Dodson-Robinson, S. E. & Salyk, C. 2011, *ApJ*, 738, 131
Ireland, M. 2012, *in Proc. SPIE* Vol. 8447, 79
Ireland, M. J. 2013, *MNRAS*, 433, 1718
Ireland, M. J. & Kraus, A. L. 2008, *ApJ*, 678, L59
Ireland, M. J., Monnier, J. D., & Thureau, N. 2006, *in Proc. SPIE* Vol. 6268, 58I
Kraus, A. L. & Ireland, M. J. 2012, *ApJ*, 745, 5
Lafrenière, D., Doyon, R., Marois, C., Nadeau, D., Oppenheimer, B. R., Roche, P. F., Rigaut, F., Graham, J. R., Jayawardhana, R., Johnstone, D., Kalas, P. G., Macintosh, B., & Racine, R. 2007, *ApJ*, 670, 1367
Marley, M. S., Fortney, J. J., Hubickyj, O., Bodenheimer, P., & Lissauer, J. J. 2007, *ApJ*, 655, 541
Martinache, F. 2010, *ApJ*, 724, 464
Mayor, M, & Queloz, D. 1995, *Nature*, 378, 355
Simon, M., Dutrey, A., & Guilloteau, S. 2000, *ApJ*, 545, 1034
Soummer, R., Pueyo, L., & Larkin, J. 2012, *ApJ*, 755, L28

Discussion

Chiang: Why can't reflection explain the near-infrared photometry?

Ireland: It isn't possible for reflection to give $\Delta M = 3.5$, even with an albedo of 1.0. However, the strongest argument is due to red colours: I have tried to create fake dust that would reproduce the colours, but would need the imaginary refractive index to increase by a factor of 10 between e.g. L' and K' filters. I don't think there is a physical dust type that can do this.

Chiang: Is there evidence for the time-variability in the photometry?

Ireland: Yes, especially in the K' filter. The "lobes" vary by more than a factor of 2 between epochs.

Graham: What is the speckle coherence lifetime needed?

Ireland: The exposure times are 10 to 20 seconds, much longer than any coherence time. See Ireland (2013) for details.

Graham: Comment: The median age of the GPI input sample is ≈125 Myr and therefore sensitive to the heat of formation and will distinguish between hot start/cold start, but not see the accretion spike.